Synthesis of Trioxy- and Tetraoxysilatranes with All Six-Membered Rings. Structure and Dynamic NMR Behavior[1]

Natalya V. Timosheva, A. Chandrasekaran, Roberta O. Day, and Robert R. Holmes*

Department of Chemistry, University of Massachusetts, Amherst, Massachusetts 01003-9336

Received September 25, 2000

A series of silatranes containing all six-membered rings $N[CH_2(Me_2C_6H_2)O]_3SiR$ was prepared using tris(2-hydroxy-3,5-dimethylbenzyl)amine, **7**, as the encapsulating agent in the case of **2** (CH_2Cl), **4A** ($CH{=}CH_2$), **4B** ($CH{=}CH_2$), **5** (CH_2Ph), and **6** ($CH_2CH_2(C_5H_4N)$). Silatranes **1** (OC_6H_4-4-Br) and **3** (OC_6H_4-4-CMe_3) were synthesized by transesterification of a previously known silatrane **B,** where R = OMe. Their structures were established by X-ray analyses and correlated with ^{29}Si NMR data. VT ^{1}H NMR spectra reflected fluxional behavior for all of these chiral molecules **1**−**6**. The activation energies for enantiomeric conversion of the clockwise and anticlockwise orientations of the propeller-like silatranes **1**−**6** increased as the Si−N distance decreased. This trend paralleled an increase in structural rigidity associated with the ring system as supported by ring torsional data supplied by the X-ray analyses. The degree of nitrogen donor interaction depends primarily on electronegativity effects induced at silicon by the exocyclic ligand. Also, the Si−N distances, which are shown to linearly reflect the degree of trigonal bipyramidal character, agreed with ^{29}Si chemical shifts in indicating a correspondence between the solid and solution state structures.

Introduction

We recently prepared a new class of silatranes (**A**−**D**) containing all six-membered rings,[2] which contrasts with previous work that centered on related silatranes (**E**−**H**) containing five-membered rings.[3−6] It was shown that the silatrane systems with the larger rings allowed substituent effects associated with the axial position of the resulting trigonal bipyramidal structures (TBP) to be reflected in dramatically altering the Si−N bond interactions as well as in changes of the ^{29}Si chemical shifts.[2] For example, changing the axial group from methyl in silane **A** to phenyl in silane **C** resulted in a change in the Si−N distance from 2.745(4) Å to 2.238(3) Å (average due to two independent molecules in the unit cell) for these silatranes composed of all six-membered rings.[2] A corresponding substitution in the five-membered-ring silatranes **E**[3] and **G**[5] produced a Si−N distance alteration that did not significantly change, i.e., 2.175(4) Å for the methyl-substituted silatrane **E** and 2.160(4) Å (av) for the phenyl-substituted silatrane **G**.

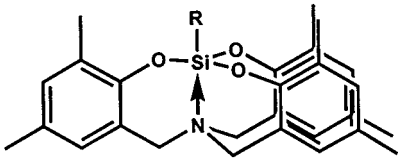

	R
A	Me
B	OMe
C	Ph
D	CCl_3

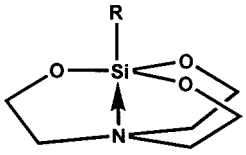

	R
E[3]	Me
F[4]	OEt
G[5]	Ph
H[6]	Cl

On comparison of the series of newly formed silatranes having the six-membered rings,[2] X-ray analysis showed a variation of over 0.7 Å in the Si−N distance, while the analogous series with five-membered rings[3−6] ranged only over 0.15 Å. It was concluded[2] that the greater rigidity imposed by the presence of five-membered rings in all previously studied silatranes[7,8]

(1) (a) Pentacoordinated Molecules 133. (b) Part 132: Chandrasekaran, A.; Day, R. O.; Holmes, R. R. Synthesis and Structure of Cyclic Phosphate, Phosphoramidate, Phosphonates and Phosphonium Salts. Atrane Formation. *Inorg. Chem*., accepted for publication.

(2) Chandrasekaran, A.; Day, R. O.; Holmes, R. R. *J. Am. Chem. Soc.* **2000**, *122*, 1066.

(3) Parkanyi, L.; Bihatsi, L.; Henesei, P. *Cryst. Struct. Commun.* **1978**, *7*, 435.

(4) Grant, R. J.; Daniels, L. M.; Das, S. K.; Janakiraman, M. N.; Jacobson, R. A.; Verkade, J. G. *J. Am. Chem. Soc.* **1991**, *113*, 5728.

(5) (a) Turley, J. W.; Boer F. P. *J. Am. Chem. Soc.* **1968**, *90*, 4026. (b) Parkanyi, L.; Simon, K.; Nagy, J. *Acta Crystallogr.* **1974**, *B30*, 2328. (c) Parkanyi, L.; Nagy, J.; Simon, K. *J. Organomet. Chem.* **1975**, *101*, 11.

(6) Kemme, A. A.; Bleidelis, J. J.; Pestunovich, V. A.; Baryshok, V. P.; Voronkov, M. G. *Dokl. Akad. Nauk SSSR* **1978**, *243*, 688; *Chem. Abstr.* 90:86560, 1979.

10.1021/om0008225 CCC: $19.00
Publication on Web 11/21/2000

limited the extent of Si−N interaction that could be studied by substituent variations.

Since our previous study was confined to the four silatranes (**A**−**D**), we report here a more extensive series containing six-membered rings which encompasses a wider variation in ligand substitution. Both tetraoxy silanes (**1** and **3**) and monoorganotrioxy silanes (**2** and **4**−**6**) are included in the study. Their syntheses, dynamic NMR behavior in solution, and solid state structures from X-ray analyses are reported. The results are compared with the previous study of silatranes (**A**−**D**)[2] to demonstrate the consequences of increased ring flexibility in reflecting Si−N donor action controlled by substituent variations.

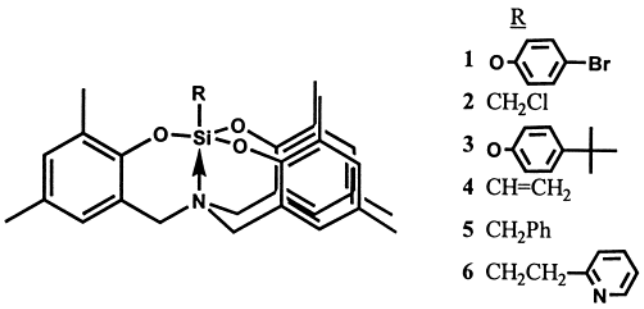

Experimental Section

Benzyltrichlorosilane, trichlorovinylsilane, chloromethyltrichlorosilane, *p*-bromophenol, *p*-*tert*-butylphenol (Aldrich), triphenoxyvinylsilane, and trimethoxy-2-(2-pyridylethyl)silane (United Chemical Technologies) were used as supplied. Tris(2-hydroxy-3,5-dimethylbenzyl)amine, $N[CH_2(Me_2C_6H_2)OH]_3$ (**7**), and methoxy silatrane **B** were synthesized using a procedure reported earlier.[2] Triethylamine (Aldrich) was distilled over KOH pellets. Solvents were purified according to standard procedures.[10] All of the reactions involving silanes were carried out in a dry nitrogen atmosphere. Proton NMR spectra were recorded on a Bruker AC200-FT-NMR spectrometer in $CDCl_3$. Silicon-29 NMR spectra were recorded on a Bruker AMX500 FT-NMR spectrometer (in CH_2Cl_2). Chemical shifts are reported in ppm, downfield positive relative to tetramethylsilane. All were recorded at around 20 °C. Variable-temperature ^{1}H NMR data were obtained in CD_2Cl_2 solution. Elemental analyses were performed by the University of Massachusetts Microanalysis Laboratory.

Syntheses. 1-(4-Bromophenoxy)sila-2,10,11-trioxa-6-aza-3,4;8,9;12,13-tris(4′,6′-dimethylbenzo)[4.4.4.0^{1,6}]-tricyclotetradecane, $N[CH_2(Me_2C_6H_2)O]_3SiO(C_6H_4$-4-Br) (1). A solution of **B** (1.00 g, 1.93 mmol) and 4-bromophenol (0.33 g, 1.91 mmol) in toluene (50 mL) was heated to reflux for 24 h. Solvent was removed from this solution and the residue recrystallized from heptane−dichloromethane (1:2, 75 mL) under a nitrogen flow; mp 227−229 °C (yield 0.60 g, 50%). ^{1}H NMR: 2.06 (s, 9H, aryl-*Me*), 2.22 (s, 9H, aryl-*Me*), 3.71 (s, 6H, N*CH*$_2$), 6.62 (s, 3H, aryl), 6.91 (s, 3H, aryl), 7.04 (d, 8.6 Hz, 2H, aryl), 7.28 (d, 8.6 Hz, 2H, aryl). ^{1}H NMR (CD_2Cl_2, 288 K): 2.04 (s, 9H, aryl-*Me*), 2.22 (s, 9H, aryl-*Me*), 3.73 (s, 6H, N*CH*$_2$), 6.66 (s, 3H, aryl), 6.92 (s, 3H, aryl), 7.02 (d, 8.8 Hz, 2H, aryl), 7.29 (d, 8.8 Hz, 2H, aryl). ^{1}H NMR (CD_2Cl_2, 190 K): 1.97 (s, 9H, aryl-*Me*), 2.16 (s, 9H, aryl-*Me*), 3.13 (d, 14.6 Hz, 3H, N*CH*$_2$), 4.41 (d, 14.6 Hz, 3H, N*CH*$_2$), 6.64 (s, 3H, aryl), 6.89 (s, 3H, aryl), 6.97 (d, 7.4 Hz, 2H, aryl), 7.25 (d, 7.4 Hz, 2H, aryl). ^{29}Si NMR: −142.5. Due to the extreme sensitivity of the compound, satisfactory elemental analyses could not be obtained.

1-Chloromethylsila-2,10,11-trioxa-6-aza-3,4;8,9;12,13-tris(4′,6′-dimethylbenzo)[4.4.4.0^{1,6}]tricyclotetradecane, $N[CH_2(Me_2C_6H_2)O]_3SiCH_2Cl$ (2). A solution of chloromethyltrichlorolsilane (1.00 mL, 8.03 mmol) in dichloromethane (50 mL) was added to a solution of **7** (3.37 g, 8.03 mmol) and triethylamine (3.40 mL, 24.4 mmol) in dichloromethane (150 mL) with stirring at room temperature over a period of 1 h. The solution was stirred for a further period of 28 h. Solvent was removed under vacuum, the residue was extracted with diethyl ether (150 mL) and filtered, and the filtrate was left under a nitrogen flow to obtain a crystalline product; mp 250−252 °C (yield 2.60 g, 66%). ^{1}H NMR: 2.21 (s, 9H, aryl-*Me*), 2.26 (s, 9H, aryl-*Me*), 3.15 (s, 2H, CH_2Cl), 3.63 (s, br, N*CH*$_2$), 6.61 (s, 3H, aryl), 6.91 (s, 3H, aryl). ^{1}H NMR (CD_2Cl_2, 290 K): 2.21 (s, 9H, aryl-*Me*), 2.24 (s, 9H, aryl-*Me*), 3.14 (s, 2H, CH_2-Cl), 3.63 (s, br, 6H, N*CH*$_2$), 6.65 (s, 3H, aryl), 6.92 (s, 3H, aryl). ^{1}H NMR (CD_2Cl_2, 205 K): 2.23 (s, 18H, aryl-*Me*), 3.08 (d, 14.1 Hz, 3H,N*CH*$_2$), 3.12 (s, 2H, CH_2Cl), 4.32 (d, 14.1 Hz, 3H, N*CH*$_2$), 6.68 (s, 3H, aryl), 6.95 (s, 3H, aryl). ^{29}Si NMR: −123.8. Anal. Calcd for $C_{28}H_{32}ClO_3NSi$: C, 68.07; H, 6.53; N, 2.83. Found: C, 67.64; H, 6.79; N, 2.77.

1-(4-*tert*-Butylphenoxy)sila-2,10,11-trioxa-6-aza-3,4;8,9;12,13-tris(4′,6′-dimethylbenzo)[4.4.4.0^{1,6}]tricyclotetradecane, $N[CH_2(Me_2C_6H_2)O]_3Si(OC_6H_4$-4-$CMe_3$) (3). A solution of **B** (0.610 g, 1.16 mmol) and 4-*tert*-butylphenol (0.170 g, 1.13 mmol) in toluene (60 mL) was heated to reflux for 24 h. Solvent was removed from this solution and the residue dissolved in heptane−dichloromethane (1:1, 80 mL) and cooled to 0 °C to obtain a crystalline product; mp 205−208 °C (yield 0.35 g, 51%). ^{1}H NMR: 1.29 (s, 9H, t-Bu), 2.04 (s, 9H, aryl-*Me*), 2.21 (s, 9H, aryl-*Me*), 3.61 (s, 6H, N*CH*$_2$), 6.64 (s, 3H, aryl), 6.87 (s, 3H, aryl), 7.11 (d, 8.6 Hz, 2H, aryl), 7.22 (d, 8.6 Hz, 2H, aryl). ^{1}H NMR (CD_2Cl_2, 290 K): 1.30 (s, 9H, t-Bu), 2.02 (s, 9H, aryl-*Me*), 2.21 (s, 9H, aryl-*Me*), 3.64 (s, 6H, N*CH*$_2$), 6.67 (s, 3H, aryl), 6.89 (s, 3H, aryl), 7.07 (d, 8.6 Hz, 2H, aryl), 7.23 (d, 8.6 Hz, 2H, aryl). ^{1}H NMR (CD_2Cl_2, 210 K): 1.30 (s, 9H, t-Bu), 1.99 (s, 9H, aryl-*Me*), 2.22 (s, 9H, aryl-*Me*), 3.18 (d, 14.5 Hz, 3H, N*CH*$_2$), 4.46 (d, 14.5 Hz, 3H, N*CH*$_2$), 6.69 (s, 3H, aryl), 6.91 (s, 3H, aryl), 7.17 (m, 4H, aryl). ^{29}Si NMR: −136.0. Anal. Calcd for $C_{37}H_{43}NO_4Si$: C, 74.84; H, 7.30; N, 2.36. Found: C, 74.65; H, 7.36; N, 2.34.

1-Vinylsila-2,10,11-trioxa-6-aza-3,4;8,9;12,13-tris(4′,6′-dimethylbenzo)[4.4.4.0^{1,6}]tricyclotetradecane, $N[CH_2(Me_2C_6H_2)O]_3SiCH{=}CH_2{\cdot}PhOH$ (4A). A solution of vinyltriphenoxysilane (1.00 mL, 2.99 mmol) and **7** (1.25 g, 2.98 mmol) in acetonitrile (150 mL) was heated to reflux for 24 h. Solvent was removed from this solution and the residue recrystallized from heptane−dichloromethane (1:2, 100 mL) under a nitrogen flow. The crystalline product was washed with pentane and dried. The crystals were found to have 1 molar equiv of a phenol molecule in all the data; mp 171−174 °C (yield 1.3 g, 77%). ^{1}H NMR: 2.20 (s, 9H, aryl-*Me*), 2.23 (s, 9H, aryl-*Me*), 3.43 (s, 6H, N*CH*$_2$), 6.09−6.57 (m, 3H, vinyl), 6.70 (s, 3H, aryl), 6.85 (s, 3H, aryl). ^{1}H NMR (CD_2Cl_2, 290 K): 2.21 (s, 9H, aryl-*Me*), 2.22 (s, 9H, aryl-*Me*), 3.40 (s, 6H, N*CH*$_2$), 6.1−6.6 (m, 3H, vinyl), 6.73 (s, 3H, aryl), 6.89 (s, 3H, aryl). ^{1}H NMR (CD_2Cl_2, 185 K): 2.21 (s, 18H, aryl-*Me*), 2.76 (d, 11.0 Hz, 3H, N*CH*$_2$), 3.95 (d, 11.0 Hz, 3H, N*CH*$_2$), 6.1−6.6 (m, 3H, vinyl), 6.74 (s, 3H, aryl), 6.89 (s, 3H, aryl). ^{29}Si NMR: −97.2. Anal. Calcd for $C_{29}H_{33}NO_3Si{\cdot}C_6H_6O$: C, 74.30; H, 6.95; N, 2.48. Found: C, 73.18; H, 7.03; N, 2.48.

(7) (a) Verkade, J. G.*Coord. Chem. Rev.* **1994**, *137*, 233. (b) Verkade, J. G. *Acc Chem. Res.* **1993**, *26*, 896. (c) Schrock, R. R. *Acc. Chem. Res.* **1997**, *30*, 9. (d) Lukevits, E.; Pudova, O. A. *Chem. Heterocycl. Compd.* **1996**, *32*, 1381.

(8) Tandura, S. N.; Voronkov, M. G.; Alekseev, N. V. *Top. Curr. Chem.* **1986**, *131*, 99.

(9) In ref 7a, p 245, Verkade reports that a series of quasi-azaphosphatranes containing five-membered rings show a similar correlation.

(10) (a) Riddick, J. A., Bunger, W. B., Eds. Organic Solvents. In *Physical Methods in Organic Chemistry*, 3rd ed.; Wiley-Interscience: New York, 1970; Vol. II. (b) Vogel, A. I. *Textbook of Practical Organic Chemistry*; Longman: London, 1978.

1-Vinylsila-2,10,11-trioxa-6-aza-3,4;8,9;12,13-tris(4′,6′-dimethylbenzo)[4.4.4.0^{1,6}]tricyclotetradecane, N[CH_2-($Me_2C_6H_2$)O]$_3$SiCH=CH_2·1/2Et_2O (4B). A procedure similar to that for **2** was used. The quantities were as follows: **7** (3.30 g, 7.86 mmol), triethylamine (3.30 mL, 24.8 mmol), and vinyltrichlorosilane (1.00 mL, 7.86 mmol). The crystals were found to have 1/2 molar equiv of a diethyl ether molecule in all the data; mp 117−119 °C (yield 2.40 g, 65%). ^{1}H NMR: 2.20 (s, 9H, aryl-*Me*), 2.23 (s, 9H, aryl-*Me*), 3.43 (s, 6H, NCH_2), 6.09−6.57 (m, 3H, vinyl), 6.69 (s, 3H, aryl), 6.86 (s, 3H, aryl). ^{29}Si NMR: −97.2. Anal. Calcd for $C_{29}H_{33}NO_3Si\cdot{}^1/_2C_4H_{10}O$: C, 73.19; H, 7.53; N, 2.75. Found: C, 72.83; H, 7.38; N, 2.76.

1-Benzylsila-2,10,11-trioxa-6-aza-3,4;8,9;12,13-tris(4′,6′-dimethylbenzo)[4.4.4.0^{1,6}]tricyclotetradecane, N[CH_2-($Me_2C_6H_2$)O]$_3$SiCH$_2$Ph·1/6C_7H_{16} (5). A procedure similar to that for **2** was used. The quantities were as follows: **7** (2.40 g, 5.72 mmol), triethylamine (2.40 mL, 17.2 mmol), and benzyltrichlorosilane (1.00 mL, 5.67 mmol). Crystals were obtained by slow evaporation from a solution of heptane−dichloromethane (1:2, 75 mL). The crystals were found to have 1/6 molar equiv of a heptane molecule in all the data; mp 128−131 °C (yield 1.50 g, 48%). ^{1}H NMR: 2.00 (s, 9H, aryl-*Me*), 2.19 (s, 9H, aryl-*Me*), 2.71 (s, 2H, CH_2Ph), 3.48 (s, 6H, NCH_2), 6.64 (s, 3H, aryl), 6.83 (s, 3H, aryl), 7.08 (m, 1H, Ph), 7.21 (t, 7.2 Hz, 2H, Ph), 7.53 (d, 6.9 Hz, 2H, Ph). ^{1}H NMR (CD_2Cl_2, 290 K): 2.02 (s, 9H, aryl-*Me*), 2.20 (s, 9H, aryl-*Me*), 2.71 (s, 2H, CH_2Ph), 3.48 (s, 6H, NCH_2), 6.68 (s, 3H, aryl), 6.86 (s, 3H, aryl), 7.08 (m, 1H, Ph), 7.22 (t, 7.9 Hz, 2H, Ph), 7.53 (d, 7.2 Hz, 2H, Ph). ^{1}H NMR (CD_2Cl_2, 180 K) 1.95 (s, 9H, aryl-*Me*), 2.12 (s, 9H, aryl-*Me*), 2.43 (s, br, 1H, CH_2Ph), 2.58 (s, br, 1H, CH_2Ph), 2.83 (br, 3H, NCH_2), 4.07 (d, 11.0 Hz, 3H, NCH_2), 6.60 (s, 3H, aryl), 6.82 (s, 3H, aryl), 7.00 (m, 1H, Ph), 7.15 (t, 7.2 Hz, 2H, Ph), 7.45 (d, 7.2 Hz, 2H, Ph). ^{29}Si NMR: −101.3. Anal. Calcd for $C_{34}H_{37}NO_3Si\cdot1/6C_7H_{16}$: C, 76.46; H, 7.24; N, 2.54. Found: C, 76.58; H, 7.56; N, 2.43.

1-(2-Pyridylethyl)sila-2,10,11-trioxa-6-aza-3,4;8,9;12,13-tris(4′,6′-dimethylbenzo)[4.4.4.0^{1,6}]tricyclotetradecane, N[CH_2($Me_2C_6H_2$)O]$_3$SiCH$_2$CH$_2$(C_5H_4N) (6). A procedure similar to that for **4A** was used. The quantities were as follows: **7** (1.85 g, 4.41 mmol), 2-(2-pyridylethyl)trimethoxysilane (1.00 mL, 4.40 mmol), and catalyst tetraethylammonium fluoride·*x*H_2O (0.1 g). On cooling to room temperature, crystals formed; mp 180−181 °C (yield 1.90 g, 78%). ^{1}H NMR: 1.56 (m, 2H, $SiCH_2$), 2.21 (s, 9H, aryl-*Me*), 2.29 (s, 9H, aryl-*Me*), 3.32 (m, 2H, CH_2Py, Py = pyridyl), 3.48 (s, 6H, NCH_2), 6.68 (s, 3H, aryl), 6.87 (s, 3H, aryl), 7.12 (m, 1H, Py), 7.27 (d, 8.2 Hz, 1H, Py), 7.63 (td, 7.2 Hz, 1.8 Hz, 1H, Py), 8.59 (m, 1H, Py). ^{1}H NMR (CD_2Cl_2, 290 K): 1.54 (m, 2H, $SiCH_2$), 2.21 (s,9H, aryl-*Me*), 2.29 (s, 9H, aryl-*Me*), 3.30 (m, 2H, CH_2Py, Py = pyridyl), 3.47 (s, 6H, NCH_2), 6.73 (s, 3H, aryl), 6.90 (s, 3H, aryl), 7.12 (m, 1H, Py), 7.28 (d, 7.6 Hz, 1H, Py), 7.62 (m, 1H, Py), 8.53 (m, 1H, Py). ^{1}H NMR (CD_2Cl_2, 180 K): 1.30 (br, 2H, $SiCH_2$), 2.14 (s, br, 18H, aryl-*Me*), 2.82 (br, 3H, NCH_2), 3.15 (br, 2H, CH_2Py, Py = pyridyl), 4.02 (br, 3H, NCH_2), 6.62 (s, 3H, aryl), 6.84 (s, 3H, aryl), 7.13 (m, 1H, Py), 7.27 (br, 1H, Py), 7.66 (br, 1H, Py), 8.49 (br, 1H, Py). ^{29}Si NMR: −91.3. Anal. Calcd for $C_{34}H_{38}N_2O_3Si$: C, 74.15; H, 6.95; N, 5.09. Found: C, 73.64; H, 6.93; N, 5.41.

X-ray Studies. The X-ray crystallographic studies were performed using an Enraf-Nonius CAD4 diffractometer and graphite-monochromated Mo Kα radiation (=0.71073 Å). Details of the experimental procedures have been described previously.[11]

The colorless crystals were mounted in thin-walled glass capillaries which were sealed to protect the crystals from the atmosphere as a precaution. Data were collected at 23 ± 2 °C using the $\theta-2\theta$ scan mode with $4° \le 2\theta_{MoK\alpha} \le 44°$. Absorption corrections were applied only for **1** using 2 sets of ψ data (T_{min}/T_{max} = 0.83). All of the data with positive intensities were included in the refinement. The structures were solved by direct methods and difference Fourier techniques and were

Table 1. Crystallographic Data for Compounds 1−6

	1	2	3	4A	4B	5	6
formula	$C_{33}H_{34}BrNO_4Si$	$C_{28}H_{32}ClNO_3Si$	$C_{37}H_{43}NO_4Si$	$C_{29}H_{33}NO_3Si\cdot C_6H_6O$	$C_{29}H_{33}NO_3Si\cdot1/2C_4H_{10}O$	$C_{34}H_{37}NO_3Si\cdot1/6C_7H_{16}$	$C_{34}H_{38}N_2O_3Si$
fw	616.6	494.09	593.81	565.76	508.71	552.44	550.75
cryst syst	monoclinic	monoclinic	monoclinic	rhombohedral	rhombohedral	rhombohedral	triclinic
space group	$P2_1/c$	$P2_1/c$	$P2_1/n$	$R\bar{3}$	$R\bar{3}$	$R\bar{3}$	$P\bar{1}$
cryst size, mm	0.47 × 0.35 × 0.25	0.75 × 0.75 × 0.50	1.00 × 0.50 × 0.50	1.00 × 0.55 × 0.55	0.90 × 0.50 × 0.40	0.65 × 0.50 × 0.50	1.00 × 0.50 × 0.30
a (Å)	10.147(4)	18.370(6)	10.822(3)	14.016(4)	13.804(5)	24.692(5)	12.831(3)
b (Å)	17.207(6)	17.526(14)	15.463(3)	14.016(5)	13.804(5)	24.692(4)	16.835(8)
c (Å)	17.538(5)	18.895(6)	19.830(5)	26.471(8)	26.494(9)	27.536(6)	17.256(8)
α (deg)	90	90	90	90	90	90	116.19(4)
β (deg)	103.11(2)	118.02(2)	96.03(3)	90	90	90	99.64(3)
γ (deg)	90	90	90	120	120	120	106.89(3)
V (Å^3)	2982(2)	5370(5)	3300.0(14)	4504(3)	4372(3)	14539(5)	3005(2)
Z	4	8	4	6	6	18	4
D_{calc} (g/cm^3)	1.373	1.222	1.195	1.252	1.159	1.136	1.217
$\mu_{MoK\alpha}$ (cm^{-1})	14.57	2.16	1.11	1.18	1.13	1.06	1.15
total no. of reflns	3638	6557	4041	1417	1383	4287	7337
no. of reflns with $I > 2\sigma_I$	1610	3343	2535	976	844	1936	5311
R^a	0.1025	0.0628	0.0487	0.0419	0.0502	0.0636	0.0650
$R_w{}^b$	0.2144	0.1560	0.1227	0.1224	0.1394	0.1818	0.1890

^{a} $R = \sum||F_o| - |F_c||/\sum|F_o|$. ^{b} $R_w(F_o^2) = \{\sum w(F_o^2 - F_c^2)^2/\sum wF_o^4\}^{1/2}$.

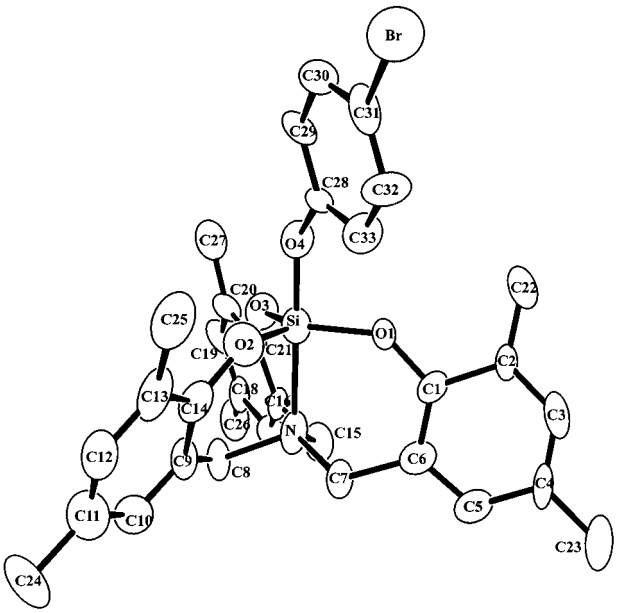

Figure 1. ORTEX diagram of **1**.

refined by full-matrix least-squares. Refinements were based on F^2, and computations were performed on a 600 MHz Pentium III computer using SHELXS-86 for solution[12] and SHELXL-93 for refinement.[13] All of the non-hydrogen atoms, except those of solvents, were refined anisotropically. Hydrogen atoms were included in the refinement as isotropic scatterers riding in either ideal positions or with torsional refinement (in the case of methyl and hydroxyl hydrogen atoms) on the bonded atoms. In the case of disordered moieties described below, the hydrogens on the disordered atoms and the adjacent atom could not be included in the calculations. The final agreement factors are based on the reflections with $I \geq 2\sigma_I$. Crystallographic data are summarized in Table 1.

There were two independent molecules in the lattice of **2**. The chlorine atom of the second molecule was disordered and was refined in two positions with 0.85:0.15 occupancies. In the lattice of **4A**, there was a disordered phenol molecule placed around the 3-fold axis, which resulted in three positions for the oxygen atom. In the lattice of **4B**, there was a disordered molecule of diethyl ether with the oxygen atom at the inversion center. In the lattice of **5** there was a highly disordered heptane molecule around the inversion center which was a 3-fold axis junction, the atoms of which were refined with 1/6 occupancies each. In the lattice of **6**, there were two independent molecules. The pyridine ring of the second molecule was disordered and was refined with equal occupancies with a hexagonal restraint.

Results and Discussion

The atom labeling schemes for **1**−**6** are given in the ORTEX[14] plots of Figures **1**−**6**, respectively. The thermal ellipsoids are shown at the 40% probability level, and all hydrogen atoms are omitted for clarity. Selected bond parameters are given in Tables 2−8.

Syntheses. The silatranes **1**−**6** were synthesized using three different methods. Silatranes **2**, **4B**, and **5** were synthesized by the reaction of the triphenol **7** with an appropriate trichlorosilane in the presence of triethylamine. The silatranes **4A** and **6** were obtained by transesterification of triphenoxyvinylsilane and tri-

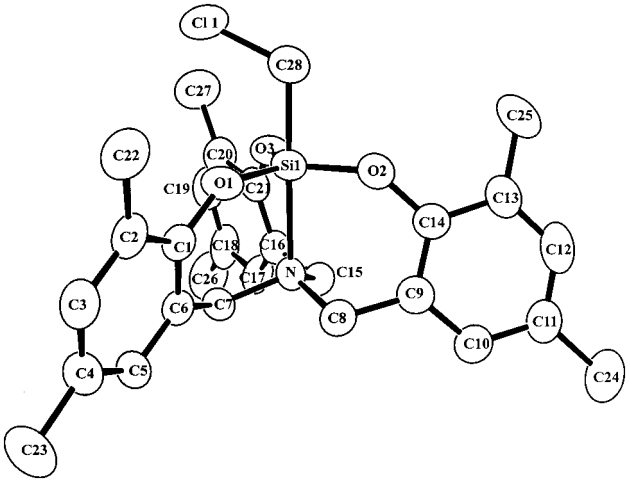

Figure 2. ORTEX diagram of **2**.

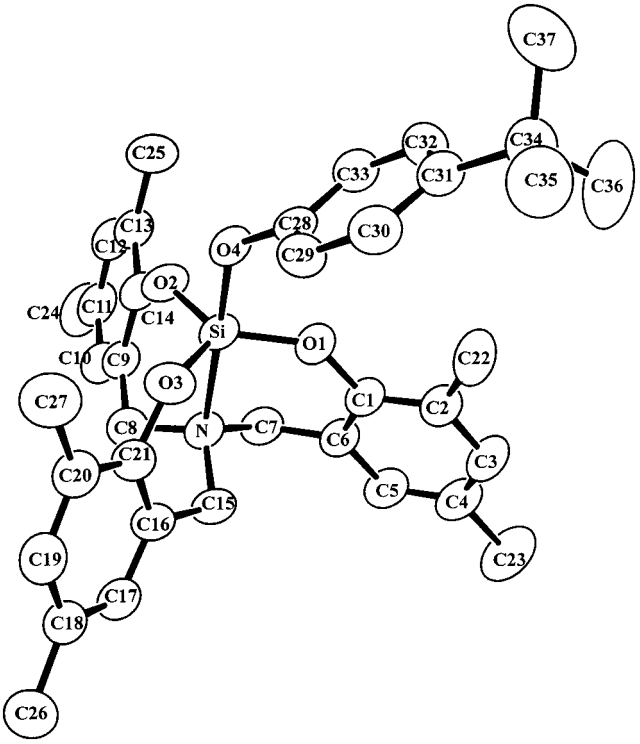

Figure 3. ORTEX diagram of **3**.

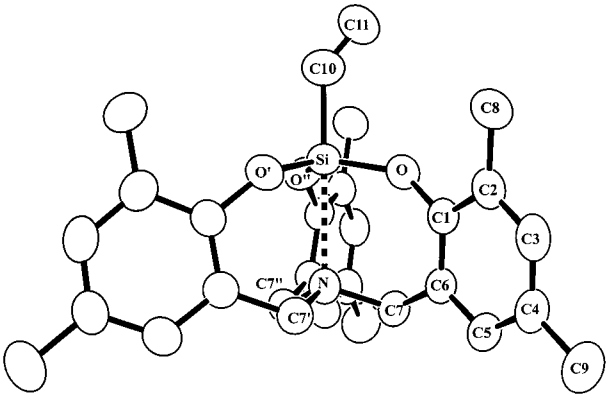

Figure 4. ORTEX diagram of **4A**. Only one of the three positions of the vinyl CH_2 carbon atom is shown.

(11) Sau, A. C.; Day, R. O.; Holmes, R. R. *Inorg. Chem.* **1981**, *20*, 3076.
(12) Sheldrick, G. M. *Acta Crystallogr.* **1990**, *A46*, 467.
(13) Sheldrick, G. M. *SHELXL-93*: Program for Crystal Structure Refinement; University of Gottingen: Gottingen, Germany, 1993.
(14) McArdle, P. *ORTEX 5e*; Crystallography Centre, Chemistry Department, University College Galway: Galway, Ireland, 1996.

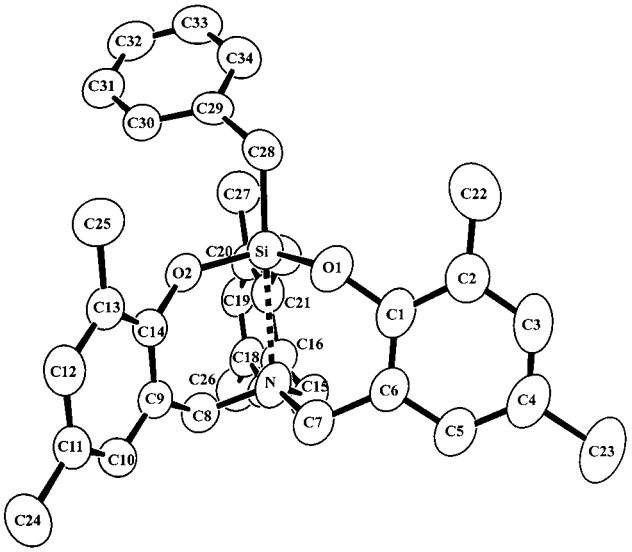

Figure 5. ORTEX diagram of **5**.

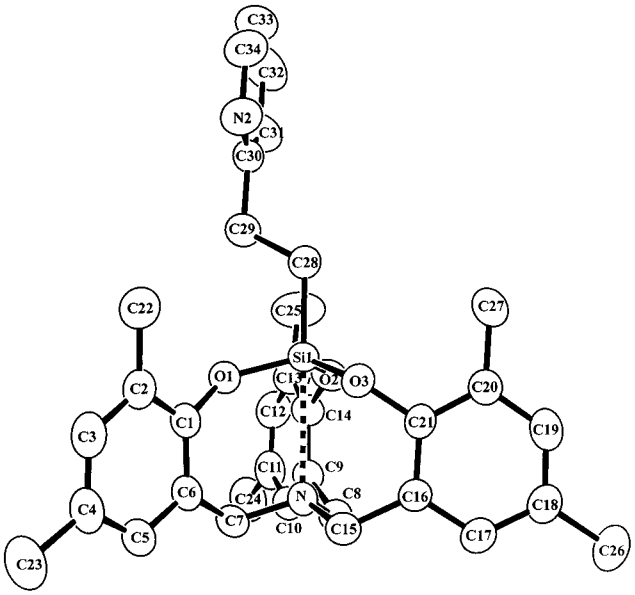

Figure 6. ORTEX diagram of **6**.

Table 2. Selected Bond Lengths [Å] and Angles [deg] for 1

Si−O(1)	1.653(9)	Si−O(4)	1.652(10)
Si−O(2)	1.608(11)	Si−N	2.111(13)
Si−O(3)	1.677(9)	Br−C(31)	1.923(14)
O(1)−Si−O(2)	119.7(5)	C(1)−O(1)−Si	138.0(10)
O(1)−Si−O(3)	119.5(5)	C(14)−O(2)−Si	140.8(10)
O(1)−Si−O(4)	93.8(5)	C(21)−O(3)−Si	137.4(10)
O(2)−Si−O(3)	120.1(5)	C(28)−O(4)−Si	129.0(9)
O(2)−Si−O(4)	93.4(5)	C(7)−N−C(8)	108.6(11)
O(3)−Si−O(4)	91.1(5)	C(7)−N−C(15)	105.9(10)
O(1)−Si−N	86.8(5)	C(8)−N−C(15)	107.4(10)
O(2)−Si−N	87.3(5)	C(7)−N−Si	112.3(9)
O(3)−Si−N	87.7(5)	C(8)−N−Si	109.5(9)
O(4)−Si−N	178.7(4)	C(15)−N−Si	112.9(9)

methoxy-2-(2-pyridyl)ethylsilane, respectively, with the triphenol **7**, whereas silatranes **1** and **3** were obtained by the transesterification of the preformed silatrane **B** with the appropriate phenol through the replacement of the methoxy group. The three methods are illustrated in eqs 1−3 for the formation of **4B**, **4A**, and **1**, respectively. All of the new silatranes **1**−**6** incorporate the

Table 3. Selected Bond Lenths [Å] and Angles [deg] for 2

Si(1)−O(1)	1.657(4)	Si(2)−O(4)	1.645(4)
Si(1)−O(2)	1.646(4)	Si(2)−O(5)	1.658(4)
Si(1)−O(3)	1.648(4)	Si(2)−O(6)	1.640(4)
Si(1)−C(28)	1.900(6)	Si(2)−C(28A)	1.933(6)
Si(1)−N(1)	2.130(5)	Si(2)−N(2)	2.112(4)
O(1)−Si(1)−O(2)	119.5(2)	O(4)−Si(2)−O(5)	120.3(2)
O(1)−Si(1)−O(3)	121.5(2)	O(4)−Si(2)−O(6)	119.6(2)
O(1)−Si(1)−C(28)	91.4(2)	O(4)−Si(2)−C(28A)	89.1(2)
O(1)−Si(1)−N(1)	87.9(2)	O(4)−Si(2)−N(2)	88.7(2)
O(2)−Si(1)−O(3)	118.7(2)	O(5)−Si(2)−O(6)	119.9(2)
O(2)−Si(1)−C(28)	90.1(2)	O(5)−Si(2)−C(28A)	92.6(2)
O(2)−Si(1)−N(1)	88.4(2)	O(5)−Si(2)−N(2)	88.3(2)
O(3)−Si(1)−C(28)	93.7(2)	O(6)−Si(2)−C(28A)	92.4(2)
O(3)−Si(1)−N(1)	88.5(2)	O(6)−Si(2)−N(2)	88.9(2)
C(28)−Si(1)−N(1)	177.8(2)	C(28A)−Si(2)−N(2)	177.8(2)
C(1)−O(1)−Si(1)	140.9(3)	C(1A)−O(4)−Si(2)	138.9(4)
C(14)−O(2)−Si(1)	139.3(4)	C(14A)−O(5)−Si(2)	139.3(3)
C(21)−O(3)−Si(1)	138.9(4)	C(21A)−O(6)−Si(2)	139.1(3)
C(7)−N(1)−C(8)	108.7(4)	C(7A)−N(2)−C(8A)	107.2(4)
C(7)−N(1)−C(15)	107.9(4)	C(7A)−N(2)−C(15A)	107.5(4)
C(7)−N(1)−Si(1)	111.2(3)	C(7A)−N(2)−Si(2)	111.2(3)
C(8)−N(1)−C(15)	108.4(4)	C(8A)−N(2)−C(15A)	109.3(4)
C(8)−N(1)−Si(1)	110.1(3)	C(8A)−N(2)−Si(2)	111.2(3)
C(15)−N(1)−Si(1)	110.5(3)	C(15A)−N(2)−Si(2)	110.2(3)

Table 4. Selected Bond Lengths [Å] and Angles [deg] for 3

Si−O(1)	1.636(3)	Si−O(4)	1.684(2)
Si−O(2)	1.638(3)	Si−N	2.166(3)
Si−O(3)	1.633(3)		
O(1)−Si−O(2)	123.0(2)	C(1)−O(1)−Si	139.2(2)
O(1)−Si−O(3)	119.9(1)	C(14)−O(2)−Si	139.3(2)
O(1)−Si−O(4)	93.3(1)	C(21)−O(3)−Si	140.3(2)
O(1)−Si−N	87.3(1)	C(28)−O(4)−Si	127.6(2)
O(2)−Si−O(3)	116.6(2)	C(7)−N−C(8)	108.6(3)
O(2)−Si−O(4)	89.5(1)	C(7)−N−C(15)	107.5(3)
O(2)−Si−N	87.5(1)	C(8)−N−C(15)	109.1(3)
O(3)−Si−O(4)	94.6(1)	C(7)−N−Si	109.9(2)
O(3)−Si−N	88.0(1)	C(8)−N−Si	110.4(2)
O(4)−Si−N	176.7(1)	C(15)−N−Si	111.2(2)

Table 5. Selected Bond Lengths [Å] and Angles [deg] for 4A

Si−O	1.635(2)	Si−N	2.542(4)
Si−C(10)	1.849(7)		
O−Si−O′[a]	117.33(4)	C(1)−O−Si	138.6(2)
O−Si−C(10)	99.51(7)	C(7)−N−C(7)′	110.0(2)
O−Si−N	80.49(7)	C(7)−N−Si	108.9(2)
C(10)−Si−N	180.0		

[a] Primed atoms were generated by $-y+1, x-y+1, z$.

triphenol **7** as the encapsulating agent. Yields ranged from 48% to 78%.

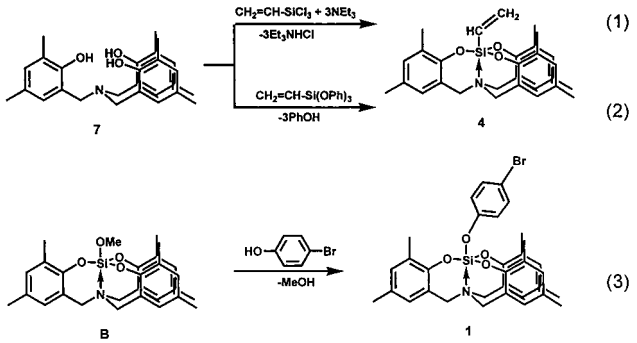

Structure. X-ray analysis shows that all six silatranes (**1**−**6**) have structures that are pentacoordinate

Table 6. Selected Bond Lengths [Å] and Angles [deg] for 4B

Si−O	1.622(2)	Si−N	2.636(4)
Si−C(10)	1.872(7)		
O−Si−O′[a]	116.07(5)	C(1)−O−Si	139.1(2)
O−Si−C(10)	101.58(8)	C(7)−N−C(7)′	110.8(2)
O−Si−N	78.42(8)	C(7)−N−Si	108.1(2)
C(10)−Si−N	180.0		

[a] Primed atoms were generated by $-y+1, x-y+1, z$.

Table 7. Selected Bond Lengths [Å] and Angles [deg] for 5

Si−O(1)	1.627(4)	Si−C(28)	1.858(6)
Si−O(2)	1.622(4)	Si−N	2.563(5)
Si−O(3)	1.618(4)		
O(1)−Si−O(2)	114.0(2)	C(1)−O(1)−Si	137.9(4)
O(1)−Si−O(3)	119.8(2)	C(14)−O(2)−Si	136.5(4)
O(1)−Si−C(28)	98.0(2)	C(21)−O(3)−Si	141.9(4)
O(1)−Si−N	79.2(2)	C(7)−N−C(8)	110.4(5)
O(2)−Si−O(3)	117.3(2)	C(7)−N−C(15)	108.9(5)
O(2)−Si−C(28)	100.7(3)	C(8)−N−C(15)	109.7(5)
O(2)−Si−N	80.1(2)	C(7)−N−Si	109.9(4)
O(3)−Si−C(28)	101.3(3)	C(8)−N−Si	108.3(3)
O(3)−Si−N	80.7(2)	C(15)−N−Si	109.6(4)
C(28)−Si−N	177.1(2)		

Table 8. Selected Bond Lengths [Å] and Angles [deg] for 6

Si(1)−O(1)	1.617(3)	Si(2)−O(1A)	1.617(3)
Si(1)−O(2)	1.620(3)	Si(2)−O(2A)	1.624(3)
Si(1)−O(3)	1.626(3)	Si(2)−O(3A)	1.614(3)
Si(1)−C(28)	1.859(4)	Si(2)−C(28A)	1.853(5)
Si(1)−N(1)	2.781(4)	Si(2)−N(1A)	2.838(4)
O(1)−Si(1)−O(2)	115.7(2)	O(1A)−Si(2)−O(2A)	111.1(2)
O(1)−Si(1)−O(3)	112.6(2)	O(1A)−Si(2)−O(3A)	111.8(2)
O(1)−Si(1)−C(28)	104.9(2)	O(1A)−Si(2)−C(28A)	105.8(2)
O(1)−Si(1)−N(1)	75.4(1)	O(1A)−Si(2)−N(1A)	74.7(1)
O(2)−Si(1)−O(3)	113.6(2)	O(2A)−Si(2)−O(3A)	115.9(2)
O(2)−Si(1)−C(28)	104.6(2)	O(2A)−Si(2)−C(28A)	105.2(2)
O(2)−Si(1)−N(1)	75.7(1)	O(2A)−Si(2)−N(1A)	74.0(1)
O(3)−Si(1)−C(28)	103.9(2)	O(3A)−Si(2)−C(28A)	106.2(2)
O(3)−Si(1)−N(1)	75.6(1)	O(3A)−Si(2)−N(1A)	74.2(1)
C(28)−Si(1)−N(1)	179.5(2)	C(28A)−Si(2)−N(1A)	179.2(2)
C(1)−O(1)−Si(1)	138.5(3)	C(1A)−O(1A)−Si(2)	132.3(3)
C(14)−O(2)−Si(1)	136.8(3)	C(14A)−O(2A)−Si(2)	132.5(3)
C(21)−O(3)−Si(1)	130.2(3)	C(21A)−O(3A)−Si(2)	135.4(3)
C(7)−N(1)−C(8)	110.5(3)	C(7A)−N(1A)−C(8A)	112.3(3)
C(7)−N(1)−C(15)	112.4(3)	C(7A)−N(1A)−C(15A)	111.8(3)
C(8)−N(1)−C(15)	110.6(3)	C(15A)−N(1A)−C(8A)	111.0(3)
C(7)−N(1)−Si(1)	108.5(2)	C(7A)−N(1A)−Si(2)	107.1(2)
C(8)−N(1)−Si(1)	108.4(2)	C(8A)−N(1A)−Si(2)	106.8(2)
C(15)−N(1)−Si(1)	106.2(2)	C(15A)−N(1A)−Si(2)	107.5(2)

and vary in their degree of trigonal bipyramidal character due to the extent of Si−N coordination. The displacement from a tetrahedral geometry toward a TBP can be judged from the silatrane bond parameters for **1**−**6** and **A**−**D** summarized in Table 9. As the nitrogen atom moves closer to silicon, indicative of increasing donor action, the R_{ax}−Si−O_{eq} angle approaches 90°. More specifically, the longest Si−N distance, 2.838(4) Å for **6**, is accompanied by an axial−equatorial angle of 105.7(2)°, which is closest to the tetrahedral angle in the series. The shortest Si−N distance is 2.025(4) Å for **D**, which has an axial−equatorial angle of 88.9(2)°, quite near the ideal TBP angle of 90°.

A plot in Figure 7 of the R_{ax}−Si−O_{eq} angle vs the Si−N distance for the series of silatranes listed in Table 9 reveals a continuous linear change in geometry toward the TBP. The diequatorial angles (O_{eq}−Si−O_{eq} in Table 9) also reflect the geometrical displacement toward an ideal TBP. This angle spans the range from 112.9(2)° to 120.0(2)° as the Si−N distance decreases from 2.838(4) Å to 2.025(4) Å. The % TBP displacement is shown in the last column. The degree of silatrane TBP character is estimated from the approach of the Si−N distance to the sum of the silicon and nitrogen covalent radii of 1.93 Å[15] relative to that for the sum of the van der Waals radii of 3.65 Å.[16]

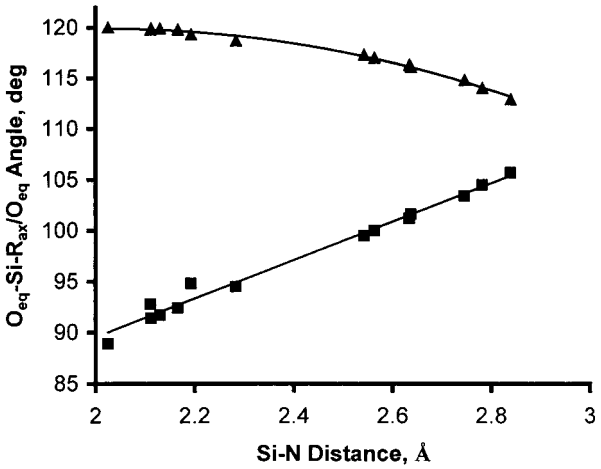

Figure 7. R_{ax}−Si−O_{eq} (■) and O_{eq}−Si−O_{eq} (▲) angles vs the Si−N distance for the silatranes listed in Table 9.

The type of correlation discussed above with reference to Table 9 and Figure 7 does not exist for previously studied silatranes,[3−9] all of which contain five-membered rings, e.g., **E**−**H**.[3−6] Due to ring constraints in over 60 of these systems, the Si−N distances found in the crystalline state are confined to a narrow range, 1.965(5)−2.240(9) Å.[7,8]

A further detail of the silatranes **1**−**6** from the X-ray analysis reveals that they all are chiral and centrosymmetric. This information will prove useful in the discussion of their dynamic NMR behavior to follow.

NMR Spectroscopy. ^{29}Si and ^{1}H NMR data are presented in Table 10 for **1**−**6** and compared with similar NMR data from our earlier study of **A**−**D**.[2] Figure 8 displays a plot of the variation in ^{29}Si chemical shift with the Si−N donor distance for these silanes. Silatranes **1**, **3**, and **B** form a series of tetraoxysilanes that differ relative to their ^{29}Si shift (lower line) compared with the monoorganotrioxysilanes (upper line). For both classes, as expected, there is a general upfield shift in the ^{29}Si value with increasing nitrogen donor coordination.

The tetraoxysilanes impart a greater Lewis acidity to the silicon atom compared with the trioxysilanes. In line with this effect, **1**, **3**, and **B** experience a greater upfield ^{29}Si shift resulting in the lower trace in Figure 8 despite the lack of a direct relationship between Lewis acidity at silicon and an upfield ^{29}Si shift in the absence of a change in coordination number. Although not perfect, the order of points for the trioxysilanes in Figure 8 corresponds to electronegativity effects induced at silicon by most of the axial substituents. This is particularly true for **D** (CCl_3 ax), which exhibits the strongest Si−N interaction, followed successively by **C**

(15) Sutton, L. *Tables of Interatomic Distances and Configuration in Molecules and Ions*; Special Publication Nos. 11 and 18; The Chemical Society: London, 1958 and 1965.
(16) Bondi, A. J. *Phys. Chem.* **1964**, *68*, 441.

Table 9. Comparison of Bond Parameters in Silatranes that Have Six-Membered Rings

compound	group R	Si−N, Å	R_{ax}−Si−N, deg	R_{ax}−Si−O_{eq},[a] deg	O_{eq}−Si−O_{eq},[a] deg	% TBP
D[b]	CCl_3	2.025(4)	178.5(2)	88.9(2)	120.0(2)	95
1	OC_6H_4-4-Br	2.111(13)	178.7(4)	92.8(5)	119.8(5)	90
2	CH_2Cl	2.112(4)	177.8(2)	91.4(2)	119.9(2)	89
		2.130(5)	177.8(2)	91.7(2)	119.9(2)	88
3	OC_6H_4-4-Bu-*t*	2.166(3)	176.7(1)	92.4(1)	119.8(2)	86
C[b]	Ph	2.193(3)	177.3(1)	94.8(2)	119.3(1)	82
		2.283(3)	176.3(1)	94.5(2)	118.7(1)	82
4A	$CH{=}CH_2$	2.542(4)	180	99.51(7)	117.33(4)	64
4B	$CH{=}CH_2$	2.636(4)	180	101.58(8)	116.07(5)	59
5	CH_2Ph	2.563(5)	177.1(2)	100.0(3)	117.0(2)	63
B[b]	OMe	2.633(6)	180	101.2(1)	116.31(7)	59
A[b]	Me	2.745(5)	180	103.36(8)	114.83(6)	53
6	CH_2CH_2-2-C_6H_4N	2.781(4)	179.5(2)	104.5(2)	114.0(2)	51
		2.838(4)	179.2(2)	105.7(2)	112.9(2)	47

[a] The angles are an average of three values except for **A**, **B**, **4A**, and **4B**. [b] Reference 2.

Table 10. Comparison of ^{29}Si and ^{1}H NMR Data for All Silatranes with Six-Membered Rings

					$\delta(NCH_2)$, ppm			
compound	group	$\Delta\gamma$, Hz	T_c, K	$\Delta G^{\ddagger}$, kcal/mol	above T_c[c]	below T_c[d]	Si−N, Å	$\delta(^{29}Si)$,[d] ppm
D[a]	CCl_3	363[b]	>363	>16.6		3.14, 4.53[c]	2.025(4)	−140.8
1[e]	OC_6H_4-4-Br	255.5	251	11.5	3.71	3.13, 4.41	2.111(13)	−142.5
2	CH_2Cl	248	258	11.8	3.63	3.08, 4.32	2.112(4)	−123.8
							2.130(5)	
3[e]	OC_6H_4-4-Bu-*t*	255.5	246	11.2	3.61	3.18, 4.46	2.166(3)	−136.0
C[a]	Ph	260	215	9.7	3.61	3.10, 4.40	2.193(3)	−110.7
							2.283(4)	
4A	$CH{=}CH_2$	237	222	10.1	3.43	2.76, 3.95	2.542(4)	−97.2
4B	$CH{=}CH_2$				3.43		2.636(4)	−97.2
5	CH_2Ph	249	206	9.3	3.49	2.83, 4.07	2.563(5)	−101.3
B[a,e]	OMe	242	230	10.4	3.50	3.07, 4.31	2.633(6)	−119.0
A[a]	Me	213	224	10.3	3.40	2.83, 3.89	2.745(5)	−74.5
6	CH_2CH_2-2-C_6H_4N	241.5	200	9.1	3.48	2.82, 4.02	2.781(4)	−91.3
							2.838(4)	

[a] Reference 2. [b] In toluene-d_8 (278.1 Hz in $CDCl_3$). [c] In $CDCl_3$. [d] In CD_2Cl_2 for ^{1}H and CH_2Cl_2 for ^{29}Si NMR. [e] These three are tetraoxysilanes, while the others are monoorganotrioxysilanes.

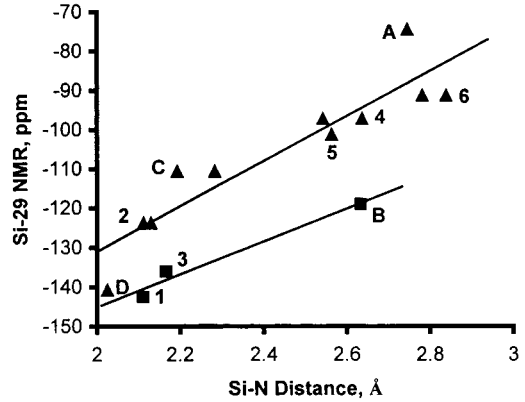

Figure 8. ^{29}Si chemical shift vs the Si−N distance for tetraoxysilatranes (■) and for monoorganotrioxysilatranes (▲).

(Ph ax), **5** (CH_2Ph ax), **6** (CH_2CH_2-2-C_6H_4N), and **A** (Me ax). Similarly, the order of increasing electronegativity of the axial groups is expressed at silicon for the tetraoxysilanes: **1** > **3** > **B**. Here, replacement of the electron-withdrawing *p*-bromo group in **1** with an electron-donating *p-tert*-butyl group to give **3** results in a decrease in the nitrogen donor interaction, while a change to an axial OMe group causes a much more substantial decrease in this interaction along with a downfield shift in the ^{29}Si value. It is also found that, in general, the increase in the Si−C ax bond in the trioxysilanes follows an order with increasing electronegativity of the axial substituent. There is insufficient data to make this conclusion for the tetraoxysilanes since only three were studied.

This is not to say that other effects are absent since we are comparing solution NMR with solid state structural data. However, lattice interactions do not appear major, as noted from the difference in Si−N distances for the two independent molecules present in the unit cell for each of the silanes **2**, **C**, and **6** and also for **4A** and **4B**, which were crystallized from different solvents. The largest difference in Si−N distances is present in **6**, which amounts to less than 0.1 Å.

Table 10 also lists variable-temperature ^{1}H NMR signals for the NCH_2 protons. As seen in Figure 9 for silanes **2** and **4A**, the spectra at low temperature comprise two doublets of equal intensity. On warming to 290 K, only a singlet is present. Thus, the signals of each of the methylene protons, which are different at low temperature and couple with each other, coalesce and time average. The process that makes the methylene protons become equivalent is most likely associated with the presence of a racemic mixture of the chiral silatranes which are rapidly intraconverting at room temperature. This applies to all of the silatranes in Table 10 other than that for **D**. As described previously, this molecule is a rigid entity. As shown in Figure 10 for **2**, the three rings most likely flip or pseudorotate simultaneously to cause the clockwise and counterclockwise propeller orientations to interchange with one another. The activation energies $\Delta G^{\ddagger}$ listed in Table 10

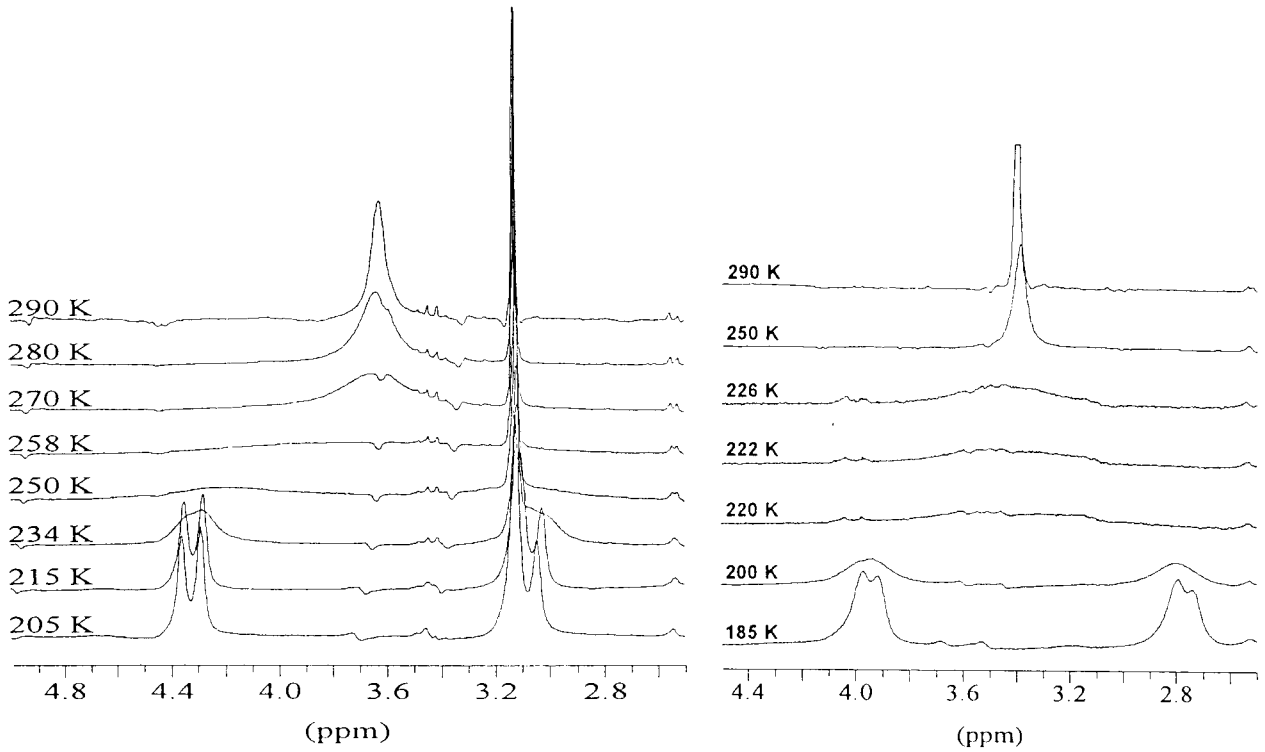

Figure 9. VT ^{1}H NMR spectra illustrating the NCH_2 proton signals for silatrane **2** (left) and for silatrane **4A** (right). An overlapping CH_2Cl signal appears at 3.12 ppm which persists over the entire temperature range studied.

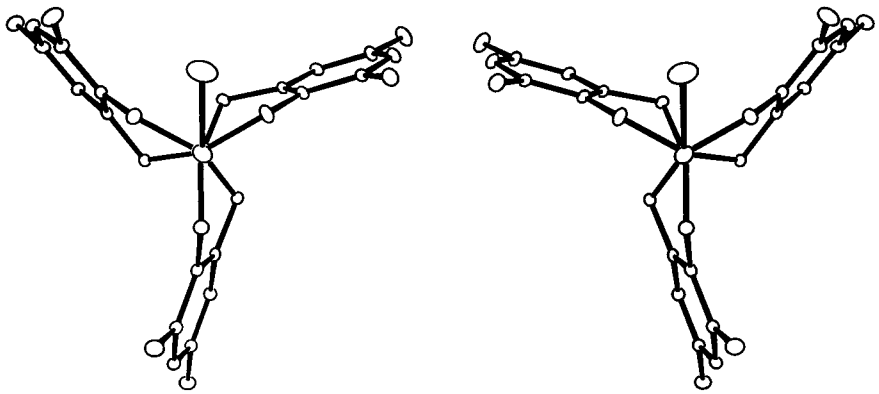

Figure 10. ORTEX diagram showing the propeller arrangements of the clockwise and anticlockwise orientations of the centrosymmetric related molecules of **2**. Both are viewed along the CH_2-Si-N axis, with CH_2Cl at the top.

are computed from eq 4.[17]

$$\Delta G^{\ddagger} = 1.987 T_c \times (23 + \log_e(T_c/\Delta\gamma)) \qquad (4)$$

There is a noticeable increase in $\Delta G^{\ddagger}$ of over 2.5 kcal/mol from **6** to **1** as the degree of nitrogen donor action increases measured by the decrease in Si−N distance. Since **D**, with the most electronegative axial group (CCl_3), is not fluxional and has the shortest Si−N distance of this series, apparently nitrogen coordination when sufficiently strong acts to inhibit the exchange process.[2]

Ring Conformations. The atoms connected to the aromatic rings of the silatranes **1**−**6** and **A**−**D** and the aromatic ring atoms themselves form nearly planar arrangements with very small variations which can safely be neglected for our considerations. Thus, the degree of distortions in this series can be evaluated by determining how far the silicon and nitrogen atoms deviate from these planes. This analysis is summarized in Table 11, where the atom deviations are expressed as distances from the mean plane formed by the O−C(Ar)−C(Ar)−C(H_2) atoms that are attached to the aromatic rings in each case. The difference in the silicon and nitrogen out-of-plane distances is used as a measure of ring distortion, with a larger difference associated with a more constrained ring system. Examination of this column of Table 11 shows that the tetraoxysilanes **1**, **3**, and **B** express increasing ring distortion that parallels decreasing Si−N distance.

For the trioxysilanes, the trend is similar except for the axial phenyl-substituted silatrane **C** in that an implied increase in ring distortion follows a decrease in Si−N distance. Figure 11 for silatranes **1**−**6** shows that as Si−N coordination decreases, the ring goes from a half-chair in **1** to a boat for **6**. In general, this analysis follows the conclusion resulting from coordination of the

(17) Williams, D. H.; Fleming, I. *Spectroscopic Methods in Organic Chemistry*, 4th ed.; McGraw-Hill: New York, 1989; p 103. The expression in eq 4 is a variation of the one reported in this reference.

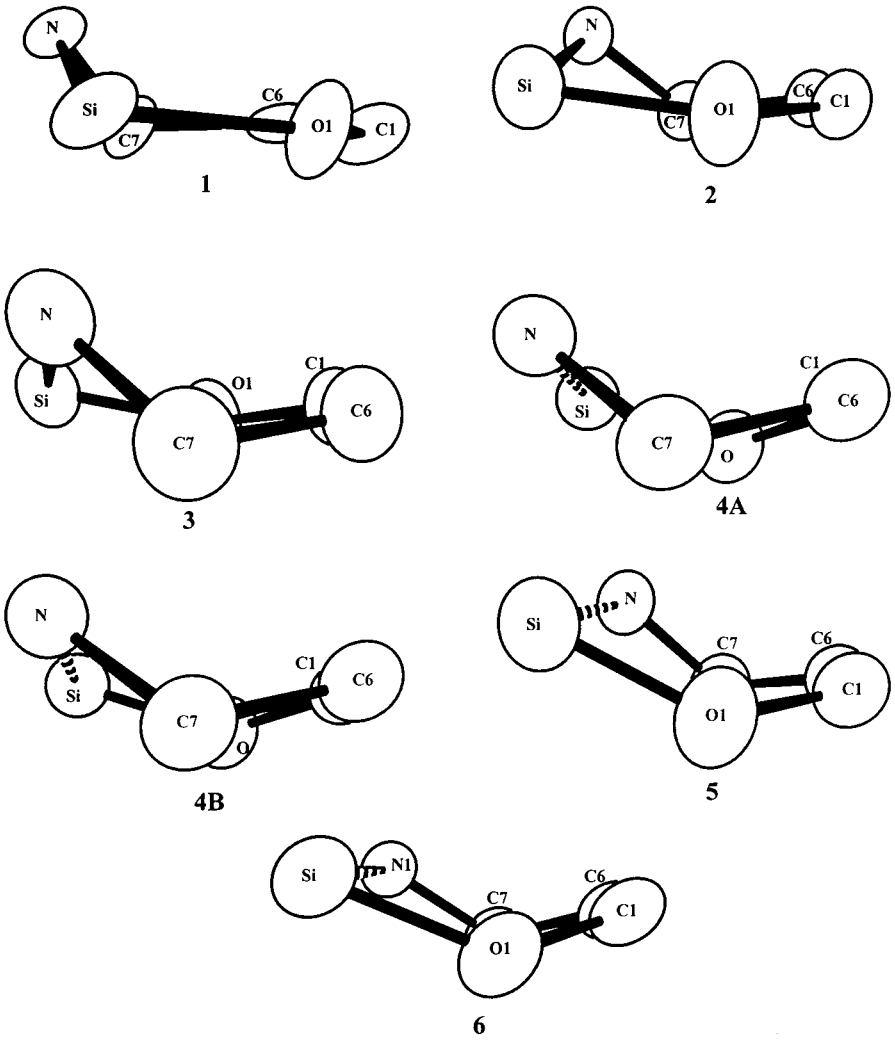

Figure 11. ORTEX diagrams of ring conformations of silatranes **1**−**6**.

Table 11. Ring Conformational Distortions of Silatranes

compound	mean deviation,[b] Å		difference in Si, N deviation, Å
	Si	N	
D	0.418(8)	0.950(8)	0.532
1[a]	0.16(2)	0.82(2)	0.660
2	0.513(8)	0.994(8)	0.481
	0.481(8)	0.980(8)	0.499
3[a]	0.506(8)	1.002(8)	0.496
C	−0.012(6)	0.815(6)	0.827
	0.068(6)	0.756(6)	0.688
4A	0.911(4)	1.129(4)	0.218
4B	0.930(4)	1.137(4)	0.207
5	0.912(8)	1.094(9)	0.182
B[a]	0.977(5)	1.142(5)	0.165
A	0.991(4)	1.152(4)	0.161
6	1.091(6)	1.116(7)	0.025
	1.143(6)	1.132(6)	−0.011

[a] These three are tetraoxysilanes, while the others are monoorganotrioxysilanes. [b] Average mean deviation from the respective O−C(Ar)−C(Ar)−C(H_2) plane of the six-membered ring involving the Si−N bond.

dynamic exchange process where the silatrane became less fluxional as the activation energy increased, culminating in a rigid molecule for **D** which contained the most electronegative axial substituent (Table 9).

Summary and Conclusion

It is clear that silatranes constructed with six-membered rings impart structural flexibility that allows substituent effects to be studied with far greater ease than that with previously studied silatranes that contained five-membered rings. This is borne out by both the wide range in Si−N distances that are observed (from X-ray structural studies) and ^{29}Si chemical shifts that readily correlate with electronic effects of attached axial substituents. Further, the increase in activation energies governing the proposed dynamic exchange process associated with propeller reorientations of the chiral silatranes with six-membered rings correlates with a decrease in Si−N distance that is readily assignable with a reduction in structural flexibility. The latter is supported by changes in ring torsional measurements from the X-ray studies.

Acknowledgment. The support of this research by the National Science Foundation is gratefully acknowledged.

Supporting Information Available: Tables of atomic coordinates, anisotropic thermal parameters, bond lengths and angles, and hydrogen atom parameters for **1**−**6**. This material is available free of charge via the Internet at http://pubs.acs.org.

OM0008225